Atmospheric Environment 309 (2023) 119926

Contents lists available at ScienceDirect

Atmospheric Environment

journal homepage: www.elsevier.com/locate/atmosenv

Assessing surface ozone risk to human health and forests over time in Poland

Arlinda Cakaj [a], Erjon Qorri [b], Fatimatou Coulibaly [c], Alessandra De Marco [d], Evgenios Agathokleous [e], Stefan Leca [f], Pierre Sicard [c,*]

[a] Poznań University of Life Sciences, Faculty of Environmental and Mechanical Engineering, Poznań, Poland
[b] Poznań University of Life Sciences, Department of Ecology and Environmental Protection, Poznań, Poland
[c] ARGANS, 06410, Biot, France
[d] ENEA Casaccia Research Center, Rome, Italy
[e] School of Applied Meteorology, NUIST, Nanjing, China
[f] INCDS, 077030, Voluntari, Romania

HIGHLIGHTS

- We calculated human health and vegetation exposure O_3 metrics for Poland.
- We calculated short-term trends for O_3 metrics over the pre-COVID19 period (2010–2019).
- We used an interpolation approach to map O_3 exposure for risk assessment.
- We found that the O3 baseline level is rising in both urban and rural areas.
- We discussed spatial distribution of levels and changes in O_3 levels.

GRAPHICAL ABSTRACT

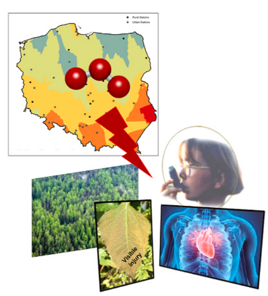

ARTICLE INFO

Keywords:
AOT40
SOMO35
Mann-Kendall test
Trend
Ozone metrics

ABSTRACT

Hourly ground-level ozone (O_3) data from 52 monitoring stations in Poland were analyzed over a ten-year pre-COVID19 period (2010–2019) to map and define areas at risk for human health and vegetation, and to calculate trends over the study period. Annual O_3 metrics (24-h average concentrations, 50th percentiles, and hourly maxima), human health metrics (Sum Of daily maximum 8-h Means Over 35 ppb, SOMO35, summertime average of the daily 8-h maximum O_3 concentrations, O_3 MDA8, and number of daily maximum 8-h values above 60 ppb, EU60) and vegetation exposure metrics (AOT40, i.e., accumulation of hourly O_3 concentrations exceeding 40 ppb during the growing season for agricultural crops AOT40c and forests AOT40f) were investigated. Higher O_3 levels occurred in rural areas than in cities. Between 2010 and 2019, the O_3 levels were rising in both urban and rural areas. Despite the reduction of nitrogen oxides (NO_x: - 2.33% year^{-1}) and volatile organic compounds emissions (VOCs: - 0.95% year^{-1}), annual O_3 mean levels (+0.81 and +0.12% year^{-1}), 50th percentiles (+1.06 and ~0% year^{-1}), hourly maxima (- 0.10 and +0.23% year^{-1}), SOMO35 (+2.86 and +1.50% year^{-1}), summertime O_3 MDA8 (+0.49 and +0.48% year^{-1}), EU60 (+0.09 and +0.15 days year^{-1}), AOT40c (+3.79 and +3.29% year^{-1}) and AOT40f (+4.47 and +4.34% year^{-1}) commonly increased in urban and rural stations. The O_3 levels increased at 75.0% of urban stations and 62.5% of rural stations. A slight decline of the number of O_3 peaks occurred in cities,

* Corresponding author.
E-mail address: psicard@argans.eu (P. Sicard).

https://doi.org/10.1016/j.atmosenv.2023.119926
Received 17 March 2023; Received in revised form 19 June 2023; Accepted 25 June 2023
Available online 26 June 2023

likely driven by the recent reductions in NO_x emissions by on-road transport. For all metrics, the increase can be attributed to higher regional photochemical O_3 formation and rising background O_3 levels likely driven by imported O_3 and its precursors by long-range transport, climate change, and lower O_3 titration by NO_x emissions decline. The failure to attain the target value for O_3 for protecting vegetation and human health and vegetation persists. Southeastern Poland, where coal stoves are still used for residential heating, faces the highest O_3 risk. This study reports new information on surface O_3 levels, exceedances, and trends in Poland to develop effective policies to mitigate O_3 effects.

1. Introduction

Nitrogen oxides (NO_x), volatile organic compounds (VOCs) and carbon monoxide (CO) are the main precursors of tropospheric ozone (O_3) (Monks et al., 2015). In terms of radiative forcing, O_3 is the third most important greenhouse gas, and contributes to climate change (IPCC, 2022). With a lifetime of several days in the boundary layer to several months in the free troposphere, O_3 can be transported from regional to hemispheric scale, influencing areas that are far from the source regions (De Marco et al., 2022). This implies that O_3 concentrations are higher in rural and remote areas downwind of urban and industrial sources of precursors emissions, i.e., in areas important for forestry, agriculture, and grassland which also support vast ecosystem services (Emberson, 2020). Tropospheric O_3 causes widespread concerns about ecosystem health and biosphere sustainability (e.g., Paoletti et al., 2019; Agathokleous E. et al., 2020,2022; Proietti et al., 2021; Sicard et al., 2021a).

Despite efforts to control O_3 precursors, the global rising background O_3 levels can be attributed to climate change leading to higher CH_4 emissions, NO_x produced by lightning, and stratospheric O_3 inputs (Sicard et al., 2017). Rising O_3 levels are observed in cities worldwide (Sicard, 2021), mainly due to reduced O_3 titration by NO (Sicard et al., 2023). Many studies have shown that surface O_3 has adverse impacts on human health (e.g., Cohen et al., 2017; Javanmardi et al., 2018; Nuvolone et al., 2018; Zhang et al., 2019), biodiversity (Agathokleous et al., 2020), natural ecosystems and crops (Mills et al., 2018), and materials (Screpanti and De Marco, 2009). Consequently, surface O_3 pollution has become a major environmental and public health concern (Malashock et al., 2022). In 2019, millions of citizens face O_3 levels above the World Health Organization (WHO) limit values for human health protection (EEA, 2020), leading to nearly 150,000 premature deaths in cities with more than 50,000 inhabitants in the world (Malashock et al., 2022).

In Europe, the European Parliament and of the Council adopted Directives on ambient air quality (e.g., Directives, 1992/72/EC, 2002/3/EC, 2008/50/EC) to regulate the air pollution such as O_3, nitrogen dioxide, sulfur dioxide, and particulate matter by setting target values and critical levels for human health and vegetation protection (EC, 2008). Following the implementation of such air quality directives and emissions control policies, the abundance of monitoring stations increased fast across Europe (Schultz et al., 2017).

In a climate change context, with rising air temperature and more frequent heat waves, a better understanding of O_3 impacts on human health and vegetation, and related trends, is still challenging for air quality management (Yan et al., 2018; Sicard et al., 2020a). Identifying surface O_3 trends is also important for assessing the efficiency of emissions control policies across Europe (Monks et al., 2015). The relative severity of exposure to O_3 can be estimated by calculating exposure metrics for human health and vegetation across a region, as well as the exceedance of critical levels (Fleming et al., 2018; Lefohn et al., 2018; Mills et al., 2018).

The ground-level O_3 trends over time are well described in the international literature (e.g., Guerreiro et al., 2014; Monks et al., 2015; Sicard et al., 2016a; Fleming et al., 2018; Yan et al., 2018; Sicard, 2021; Adame et al., 2022), except in eastern Europe, in particular Poland (Sicard, 2021). Yet 33 out of the 50 most polluted cities in the world were in Poland in 2016 (WHO, 2019). Hence, critical levels of O_3 are frequently exceeded in Poland (Wałaszek et al., 2018), leading to increased annual O_3-related number of premature deaths (+0.45 deaths per 10^6 inhabitants) between 2000 and 2017 (Sicard et al., 2021b). To summarize risk to vegetation and people, we aimed at analyzing annual surface O_3 metrics (24-h average concentrations, 50th percentile, and hourly maximum), vegetation exposure metrics (AOT40, i.e., accumulation of hourly O_3 concentrations exceeding 40 ppb for daylight hours during the growing season for crops and forests) and human health exposure metrics (SOMO35, i.e. the annual Sum Of daily maximum 8-h Means Over 35 ppb, summertime O_3 MDA8, i.e., summertime average of the daily 8-h maximum O_3 concentrations, and EU60, i.e. the number of daily maximum 8-h values above 60 ppb) at individual sites (Lefohn et al., 2018). For the first time, a ten-year analysis of surface O_3 levels and short-term annual trends were conducted at 16 rural and 36 urban stations across Poland over the time period 2010–2019. This study aims to i) produce maps of O_3 metrics for risk assessment; ii) detect and estimate the trends in O_3 metrics over time as well as in O_3 precursor emissions. In this study, we have hypothesized that the European and national precursors emissions control strategies are effective in reducing O_3 concentrations in Poland, and potential impacts on human health and vegetation.

2. Materials and methods

2.1. Data selection

The classification of stations follows the European Environment Agency guidelines, i.e., the NO-to-NO_2 ratio is used to classify stations as rural or urban background stations (Snel et al., 2004). For both urban and rural background stations, the hourly O_3 data were retrieved from the "AirBase" database of the European Environment Agency (EEA, 2020) over the time period 2010–2019. For each monitoring station, with at least 85% of validated hourly data per calendar year, we have calculated the following annual O_3 metrics: 24-h average concentration, 50th percentile, hourly maximum, human health (SOMO35, summertime O_3 MDA8, and EU60) and vegetation exposure metrics (AOT40 for crops (AOT40c) and forests (AOT40f); Mills et al., 2018). The levels of O_3 were examined over a ten-year period at 52 monitoring stations, including 16 rural and 36 urban stations, across Poland (Table 1S). From year to year, the number of background stations did not change.

To assess the efficiency of the control strategies in reducing both the emission of O_3 precursors and ground-level O_3 in Poland, the official emissions of main O_3 precursors (NO_x and non-methane VOCs) were obtained at national scale from the European Monitoring and Evaluation Program - Center on Emission Inventories and Projections for two time periods: 2005–2019 and 2010–2019. The emission data were also examined for European Union as a whole, and neighboring countries such as Belarus, Czech Republic, Russia, Slovakia, and Ukraine to account the long-range precursors transport.

2.2. Human health and vegetation exposure metrics

2.2.1. Human health metrics

The ambient air quality and Cleaner Air For Europe (CAFE) Directive 2008/50/EC (EC, 2008) has been adopted in May 2008, and sets an O_3

target concentration value of 60 ppb for the daily maximum 8-h average (abbreviated as EU60) for the protection of human health. The number of daily 8-h maximum means over 60 ppb may not exceed 25 days per calendar year (EC, 2008).

Based on the recommendation of the WHO and epidemiological studies, SOMO35 (in ppb days) is commonly used for exposure assessment and health risk for O_3 (WHO, 2008).

$$SOMO35 = \int_{i=1}^{n} \max([O_3] - 35), 0).\ dt \tag{1}$$

where $[O_3]$ is the ozone daily 8-h maximum means (ppb) exceeding 35 ppb, n is the number of days per calendar year, and dt is time step. A critical level of 3000 ppb days was suggested by Ellingsen et al. (2008).

In epidemiological studies, the highest seasonal (summertime, e.g., April–September at 45°N latitude) average daily 8-h maximum O_3 concentration (abbreviated as "summertime O_3 MDA8") is well correlated to all-causes, respiratory, and cardiovascular mortality (Turner et al., 2016). Therefore, most of epidemiological studies used the summertime O_3 MDA8 as human health-related O_3 metric (GBD, 2020), and to represent the higher O_3 exposure levels of population in urban areas (Lefohn et al., 2018). The summertime O_3 MDA8 was calculated as the annual maximum of the six-month running mean of the average daily 8-h maximum O_3 concentration.

2.2.2. Vegetation exposure metrics

AOT40f and AOT40c (in ppb hours) represent the accumulation of hourly O_3 concentrations above 40 ppb between 8 a.m. and 8 p.m. from 1st May to 31st July for any kind of (semi)natural vegetation/crops, and from 1st April to 30th September for forest trees (Mills et al., 2018).

$$AOT40 = \int_{i=1}^{n} \max(([O3] - 40), 0).\ dt \tag{2}$$

where $[O_3]$ is the hourly O_3 concentration (ppb), n is the number of hours during the assumed growing season, and dt is time step (1-h). In Europe, a critical level of AOT40c = 3000 ppb h has been established for agricultural crops (EC, 2008) and an AOT40f = 5000 ppb h is recommended for the protection of forests (UNECE, 2010).

2.3. Estimation of annual trends

To detect short-term changes within the O_3 time series, the Mann-Kendall test and Sen's slope estimator have been applied (Chattopadhyay et al., 2012; Guerreiro et al., 2014; Lefohn et al., 2018; Araminienė et al., 2019; Eghdami et al., 2022). Both non-parametric tests are robust for non-normal data distribution (Sicard et al., 2016a; Lefohn et al., 2018). For O_3 data analysis, a ten-year time-series is long enough to capture short-term trends over time likely due to changes in VOCs and NO_x emissions rather than meteorological variations (Monks et al., 2015; Sicard, 2021). Therefore, we have selected the background stations across Poland with at least 85% of validated hourly data per calendar year for ten years (2010–2019). The trends are considered as significant at $\alpha < 0.05$.

2.4. Mapping of ozone metrics

Ozone mapping is important for risk assessment as it can promote policy decisions on air quality, which in turn affect public behaviors (De Marco et al., 2022). For mapping, we used the ArcGIS 9.2 software and Geostatistical Analyst extension. The rural and urban background stations were georeferenced, and then interpolation maps were produced by considering a 100 km radius as spatial representativeness of surface O_3 data around each rural station, representative of background O_3 pollution (De Leeuw, 2000), and 5.5 km radius for each urban station (Kracht et al., 2017). The co-kriging was executed with a so-called Gaussian semivariogram model and 10 lags (lag size = 0.1), with no anisotropy and 2nd order trend removal for station data. Due to the heterogeneous geographical distribution of the O_3 monitoring stations, interpolation maps were generated using 4 nearby stations.

3. Results

3.1. Annual ozone metrics in Poland

By joining annual data from the 16 rural and 36 urban stations over the time period 2010–2019, the annual 24-h average O_3 concentrations was 27.9 ± 4.4 ppb at rural stations and 23.3 ± 2.2 ppb at urban stations (Table 1). The highest annual O_3 mean concentration occurred in 2018 at rural stations (29.1 ppb) and in 2019 at urban stations (24.8 ppb), while the lowest annual O_3 mean level was observed at rural (25.8 ppb) and urban stations (21.8 ppb) in 2014 (Tables 2S–3S). Similarly, the averaged 50th percentile of O_3 concentrations was higher at rural stations (26.8 ± 4.7 ppb) than urban stations (22.1 ± 2.8 ppb). The annual 50th percentiles ranged from 24.4 ppb in 2014 to 27.7 ppb in 2018 at rural stations and from 20.4 ppb in 2016 to 24.0 ppb in 2019 at urban stations. Between 2010 and 2019, the annual average of hourly maxima of O_3 were higher at rural stations (81.4 ± 4.1 ppb) than urban stations (78.9 ± 5.7 ppb) reaching 109.0 ppb in 2010 at urban stations and 106.3 ppb in 2015 at rural stations.

Between 2010 and 2019, the averages of O_3 exposure metrics were higher at rural stations and lower at urban stations (Table 1): SOMO35 (2440 ± 603 vs. 1764 ± 436 ppb days), summertime O_3 MDA8 (57.2 ± 2.8 vs. 53.9 ± 3.7 ppb), EU60 (18.5 ± 8.1 vs. 11.3 ± 6.1 days), AOT40c (6910 ± 1404 vs. 5433 ± 1819 ppb h) and AOT40f (12,221 ± 2515 vs. 9247 ± 3033 ppb h). The SOMO35 ranged from 1818 to 3074 ppb days at rural stations, while at urban stations SOMO35 ranged from 1426 to 2251 ppb days. The highest and lowest SOMO35 values were recorded in 2018 and 2017 at both rural and urban stations, respectively

Table 1
National-averaged ozone metrics and annual trends magnitude, with standard deviation, calculated by joining annual data from 16 rural and 36 urban stations over the time period 2010–2019: annual average ozone concentrations (annual mean), 50th percentiles (median) and hourly maxima of hourly average concentrations (hourly max.) over 24-h period, Sum Of daily maximum 8-h Means Over 35 ppb, (SOMO35), summertime average daily 8-h maximum ozone concentrations (summertime O_3 MDA8), numbers of days in which the ozone concentrations were over 60 ppb in at least one *8*-h period (EU60), and sum of the hourly ozone concentrations exceeding 40 ppb for daylight hours during the growing season for vegetation (AOT40v) and forests (AOT40f). The trend magnitudes are significant at $p < 0.05$.

Ozone metrics	Rural sites (n = 16)		Urban sites (n = 36)	
	Average	Trend	Average	Trend
Annual mean	27.9 ± 4.4 ppb	+0.12 ± 0.96% year^{-1}	23.3 ± 2.2 ppb	+0.81 ± 1.05% year^{-1}
50th percentile	26.8 ± 4.7 ppb	+0.02 ± 0.99% year^{-1}	22.1 ± 2.8 ppb	+1.06 ± 1.40% year^{-1}
Hourly max.	81.4 ± 4.1 ppb	+0.23 ± 1.14% year^{-1}	78.9 ± 5.7 ppb	- 0.10 ± 0.86% year^{-1}
SOMO35	2440 ± 603 ppb days	+1.50 ± 4.57% year^{-1}	1764 ± 436 ppb days	+2.86 ± 4.25% year^{-1}
O_3 MDA8	57.2 ± 2.8 ppb	+0.48 ± 1.03% year^{-1}	53.9 ± 3.7 ppb	+0.49 ± 0.86% year^{-1}
EU60	18.5 ± 8.1 days	+0.15 ± 1.45 days year^{-1}	11.3 ± 6.1 days	+0.09 ± 0.71 days year^{-1}
AOT40c	6910 ± 1404 ppb h	+3.29 ± 5.29% year^{-1}	5433 ± 1819 ppb h	+3.79 ± 6.79% year^{-1}
AOT40f	12,221 ± 2515 ppb h	+4.34 ± 7.16% year^{-1}	9247 ± 3033 ppb h	+4.47 ± 6.82% year^{-1}

Table 2
National annual emissions (Gg) and trends (% per year) of main ozone precursors, non-methane volatile organic compounds (NMVOC) and nitrogen oxides ($NO_x = NO + NO_2$), obtained by the Mann-Kendall test over the time periods 2005–2019 and 2010–2019. All trend magnitudes are significant at $p < 0.05$.

	2005–2019				2010–2019			
	NMVOC		NO_x		NMVOC		NO_x	
	Mean (Gg)	% year^{-1}	Mean (Gg)	% year^{-1}	Mean (Gg)	% year^{-1}	Mean (Gg)	% year^{-1}
Poland	**755 ± 57**	**- 1.39**	**765 ± 85**	**- 2.12**	**722 ± 33**	**- 0.95**	**722 ± 70**	**- 2.33**
Belarus	302 ± 80	- 2.47	165 ± 17	- 1.46	271 ± 81	- 1.85	156 ± 13	- 1.53
Czech Republic	244 ± 18	- 0.86	233 ± 42	- 2.11	233 ± 9	- 1.20	209 ± 25	- 1.98
Russia	2482 ± 237	+1.26	2575 ± 560	- 1.50	2566 ± 234	+1.56	2216 ± 146	+1.10
Slovakia	116 ± 15	- 1.54	74 ± 16	- 2.26	107 ± 9	- 1.70	70 ± 9	- 2.01
Ukraine	306 ± 79	- 2.50	575 ± 111	- 0.96	298 ± 92	- 1.79	552 ± 83	- 1.78
E.U. (28)	7380 ± 919	- 2.27	8131 ± 1459	- 3.01	6826 ± 394	- 1.38	7271 ± 754	- 2.59

Table 3
Annual ozone mean concentrations (ppb) and annual trends obtained by Mann-Kendall test (at $p < 0.05$), with standard deviation, calculated for urban and rural monitoring stations over the time periods 2005–2014 and 2005–2018 for Germany and the United States (N: number of stations; extracted from Sicard et al., 2020a).

	Time period	N	Rural stations	N	Urban stations
France	2005–2014	44	31.4 ± 6.5	136	24.0 ± 3.8
Trend (% year^{-1})			- 0.35 ± 1.40		+1.29 ± 1.75
Germany	2005–2018	68	29.1 ± 5.5	79	21.5 ± 3.2
Trend (% year^{-1})			- 0.27 ± 0.62		+0.84 ± 0.70
Italy	2005–2014	16	33.4 ± 9.1	50	24.9 ± 4.9
Trend (% year^{-1})			- 2.18 ± 1.61		+1.73 ± 3.37
Japan	2005–2014	12	36.8 ± 8.1	55	26.8 ± 3.7
Trend (% year^{-1})			- 0.90 ± 1.60		+1.79 ± 1.30
Spain	2005–2014	53	34.6 ± 5.6	77	24.3 ± 5.7
Trend (% year^{-1})			- 0.26 ± 2.10		+2.22 ± 3.00
United Kingdom	2005–2014	22	28.5 ± 3.3	29	19.5 ± 4.5
Trend (% year^{-1})			- 2.00 ± 2.20		- 0.92 ± 1.74
United States	2005–2018	69	34.8 ± 7.1	147	27.5 ± 4.6
Trend (% year^{-1})			- 0.80 ± 0.57		+0.76 ± 1.34
Poland	**2010-2019**	**16**	**27.9 ± 4.4**	**36**	**23.3 ± 2.2**
Trend (% year^{-1})			**+ 0.12 ± 0.96**		**+ 0.81 ± 1.05**

(Tables 2S–3S). The summertime O_3 MDA8 ranged from 51.2 to 52.5 ppb (in 2017) to 58.2 and 61.3 ppb (in 2015) at urban and rural stations, respectively. The EU60 ranged from 7.4 days in 2017 to 28.7 days in 2018 at rural stations and from 7.4 days in 2014 to 21.5 days in 2015 at urban stations. The AOT40c values at rural stations ranged from 4753 ppb h in 2017 to 9770 ppb h in 2018, while at urban stations the AOT40c values ranged from 4439 ppb h in 2017 to 7500 ppb h in 2018 (Tables 2S–3S). The range of AOT40f values at rural stations was 7639-17,196 ppb h, and 6951-13,002 ppb h at urban stations.

3.2. Mapping of surface ozone levels for risk assessment

The annual O_3 mean concentrations were higher in rural areas in Southern Poland at mountainous stations in southwest (Fig. 1S), e.g., in Śnieżka (1600 m a.s.l.) and Czerniawa (650 m a.s.l.) with annual levels exceeding 35 ppb (Fig. 1a). Lower O_3 levels were recorded in urban areas, e.g., in Tarnów (southeast), Warsaw (central Poland), and Katowice (south) with annual levels below 20 ppb. The lowest 50th percentiles (<20 ppb) were recorded in well-industrialized cities in the South and in Warsaw (center), while the highest values (>35 ppb) were recorded in mountainous areas in southwest Poland (Fig. 2a). The hourly maxima were generally lower in the North (<75 ppb) and higher (>85 ppb) in the South of Poland (Fig. 3a). The lowest hourly maxima were recorded in rural areas, such as in Borsukowizna (northeast) and Diabla Góra (north), with hourly maxima lower than 75 ppb. In rural stations of southern Poland, the hourly maxima reached about 85 ppb in Złoty Potok and Krzyżówka. The highest hourly maxima (>90 ppb) were observed in well-urbanized and industrialized areas in Southern Poland e.g., nearby Katowice (Fig. 3a).

For the protection of human health, the SOMO35 (Fig. 4a), summertime O_3 MDA8 (Fig. 5a), and EU60 (Fig. 6a) values were generally lower in northwest and higher in southwest of Poland over the time period 2010–2019. The lowest SOMO35 values (Fig. 4a) were recorded in urban areas in northwest Poland (Gdansk and Gdynia, <1000 ppb days), while the highest values were observed in southwest Poland in both rural (Śnieżka and Czerniawa, >4000 ppb days) and urban areas (Cieszyn and Wałbrzych, ~2500 ppb days). The highest seasonal average daily 8-h maximum O_3 concentration (>55 ppb) were observed in both rural and urban areas, in particular in industrialized areas in Southern Poland e.g., nearby Katowice (Fig. 5a). The lowest EU60 (<5 days) were observed in the cities in northern Poland (Gdansk and Gdynia) while the maximum EU60 (>25 days) values were recorded in rural areas in southwestern Poland, particularly at mountainous stations (e.g., Śnieżka), and downwind of well-urbanized areas nearby Kraków in southern Poland and Poznań in central Poland (Fig. 6a).

The spatial distribution of vegetation impact metrics (Figs. 7a–8a) is similar to human health metrics, i.e., generally lower in the North and higher in the South of Poland in both rural and urban areas. Indeed, the lowest AOT40c (<4000 ppb h) and AOT40f (<5000 ppb h) values were recorded in urban areas in northwestern Poland while the largest values (AOT40c > 7000 ppb h; AOT40f > 12,000 ppb h) were observed in rural areas at mountainous stations (above 800 m a.s.l.) in southwestern Poland and downwind of urbanized areas nearby Katowice and Kraków in Southern Poland, and Poznań in central Poland.

3.3. Trends in ozone precursor emissions

In the European Union, the NO_x and non-methane VOCs (NMVOCs) declined respectively by 2.59% year^{-1} and 1.38% year^{-1} over the time period 2010–2019 (Table 2). In Poland, significant reductions ($p < 0.05$) were observed, i.e., 0.95% year^{-1} for NMVOCs and 2.3% year^{-1} for NO_x between 2010 and 2019. The road transport-related NO_x and NMVOCs emissions declined by 0.75% year^{-1} and 3.96% year^{-1} over the time period 2010–2019, while the NMVOCs from industry sector increased by 2.53% year^{-1} (data not shown). Except for Russia, we found significant declines of O_3 precursor emissions, specifically 1.20–1.85% year^{-1} for NMVOCs and 1.53–2.01% year^{-1} for NO_x, in neighboring countries (Belarus, Czech Republic, Slovakia, and Ukraine). In Russia, the emissions of NMVOCs (+1.56% year^{-1}) and NO_x (+1.10% year^{-1}) increased over the time period 2010–2019 (Table 2).

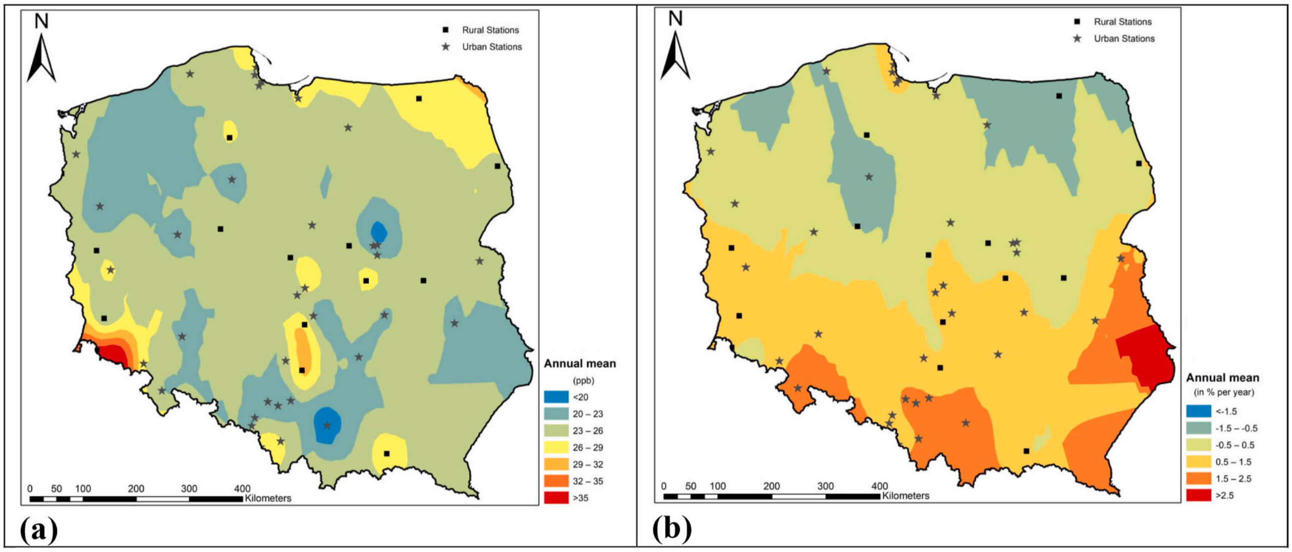

Fig. 1. Annual ozone mean concentrations (a) and annual trend magnitude (b) calculated by joining annual data from 16 rural and 36 urban stations over the time period 2010–2019.

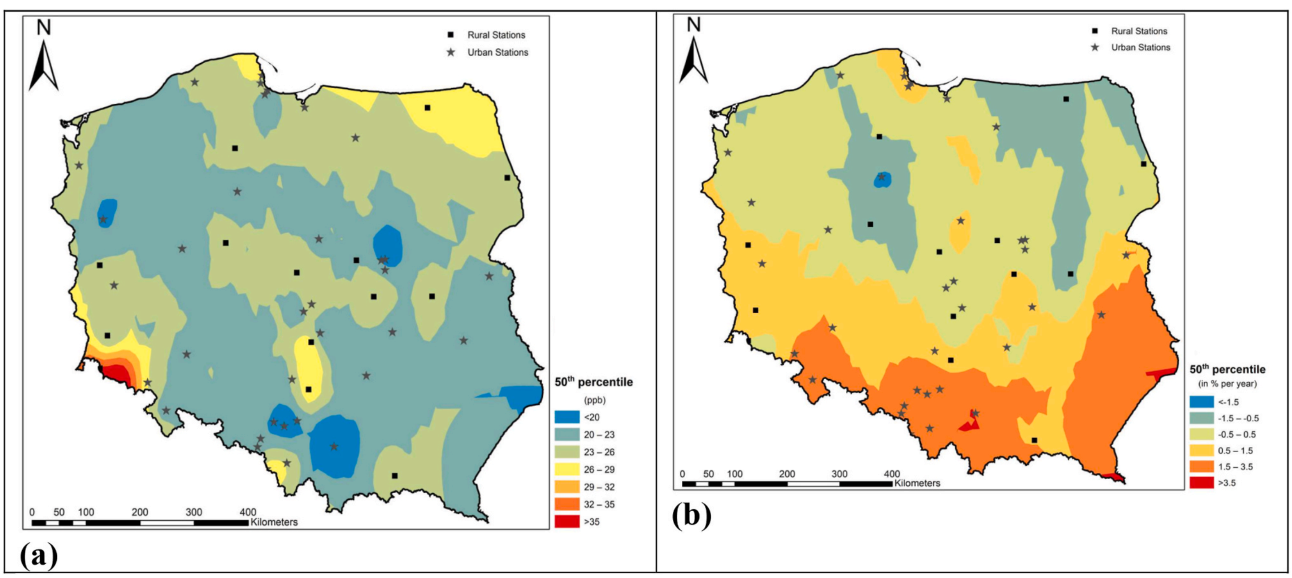

Fig. 2. Annual 50th percentiles of ozone concentrations (a) and annual trend magnitude (b) calculated by joining annual data from 16 rural and 36 urban stations over the time period 2010–2019.

3.4. Surface ozone metrics over time

At rural stations, the annual O_3 mean concentrations significantly increased by 0.12% year^{-1} between 2010 and 2019 (Table 1), and upward trends were also observed for hourly maxima (+0.23% year^{-1}) and slightly for 50th percentiles (+0.02% year^{-1}). The human health and vegetation impact metrics SOMO35 (+1.50% year^{-1}), summertime O_3 MDA8 (+0.48% year^{-1}), EU60 (+0.15 days year^{-1}), AOT40c (+3.29% year^{-1}) and AOT40f (+4.34% year^{-1}) are also rising over the study period. At urban stations, mean concentrations and 50th percentiles displayed an upward trend (+0.81 and + 1.06% year^{-1}, respectively) while slight downward trend was observed for hourly maxima (- 0.10% year^{-1}). In urban areas, SOMO35 (+2.86% year^{-1}), summertime O_3 MDA8 (+0.49% year^{-1}), EU60 (+0.09 days year^{-1}), AOT40c (+3.79% year^{-1}), and AOT40f (+4.47% year^{-1}) have significantly increased during the study period, to levels considerably higher than at rural stations (Table 1).

At national scale, the annual O_3 mean concentrations are declining (less than - 1.0% year^{-1}) in northern Poland and are rising (more than + 1.5% year^{-1}) in southeast Poland in both rural and urban stations (Fig. 1b). At rural stations, the trends in O_3 mean concentrations ranged from - 1.37% year^{-1} in Diabla Góra (north) to + 1.86% year^{-1} in Osieczów in southwest (Tables 2S–3S). At urban stations, the trends ranged from - 1.54% year^{-1} in Bydgoszcz (north) to + 2.91% year^{-1} in Kraków (southeast). Similarly, the 50th percentile of O_3 concentrations are declining (less than - 1.0% year^{-1}) in northern Poland and are rising (more than + 2.0% year^{-1}) in southeast Poland (Fig. 1b). In rural areas, the trends in 50th percentiles ranged from - 1.55% year^{-1} in Diabla Góra (north) to + 2.05% year^{-1} in Osieczów in southwest (Tables 2S–3S). In cities, the trends ranged from - 2.19% year^{-1} in Bydgoszcz (north) to + 4.15% in Kraków (southeast). At rural and urban stations, the hourly maxima are decreasing (less than - 1.0% year^{-1}) in northeast and in the South nearby Kraków and are rising (more than + 1.5% year^{-1}) in southeast and western Poland (Fig. 3b). In rural areas, the trends in

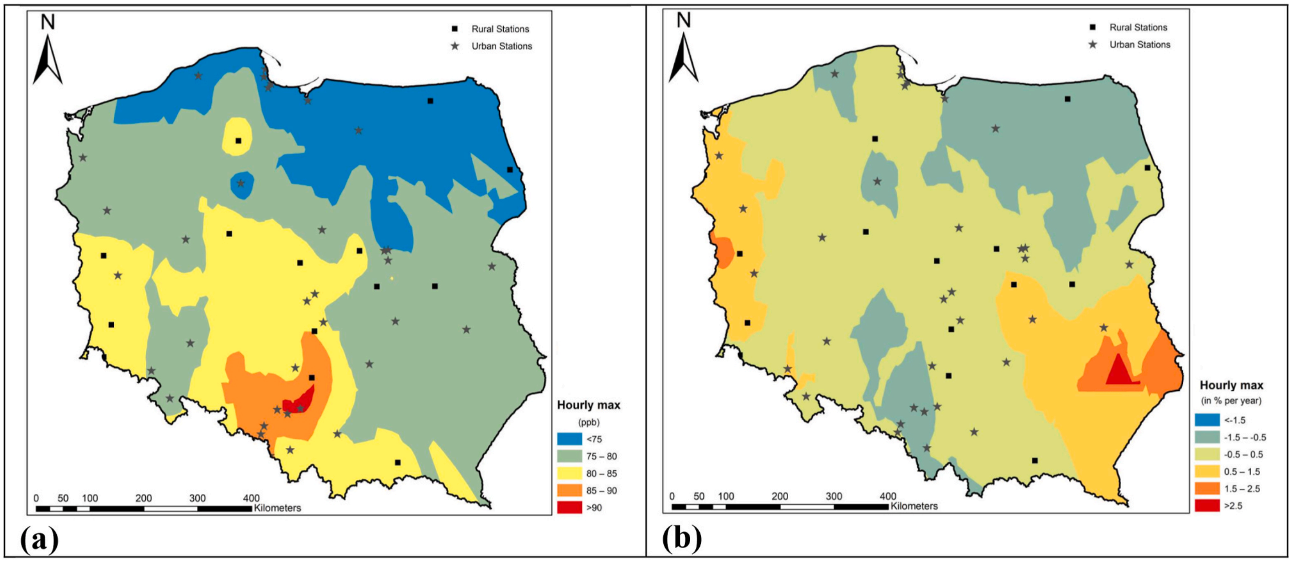

Fig. 3. Hourly maxima ozone concentrations (a) and annual trend magnitude (b) calculated by joining annual data from 16 rural and 36 urban stations over the time period 2010–2019.

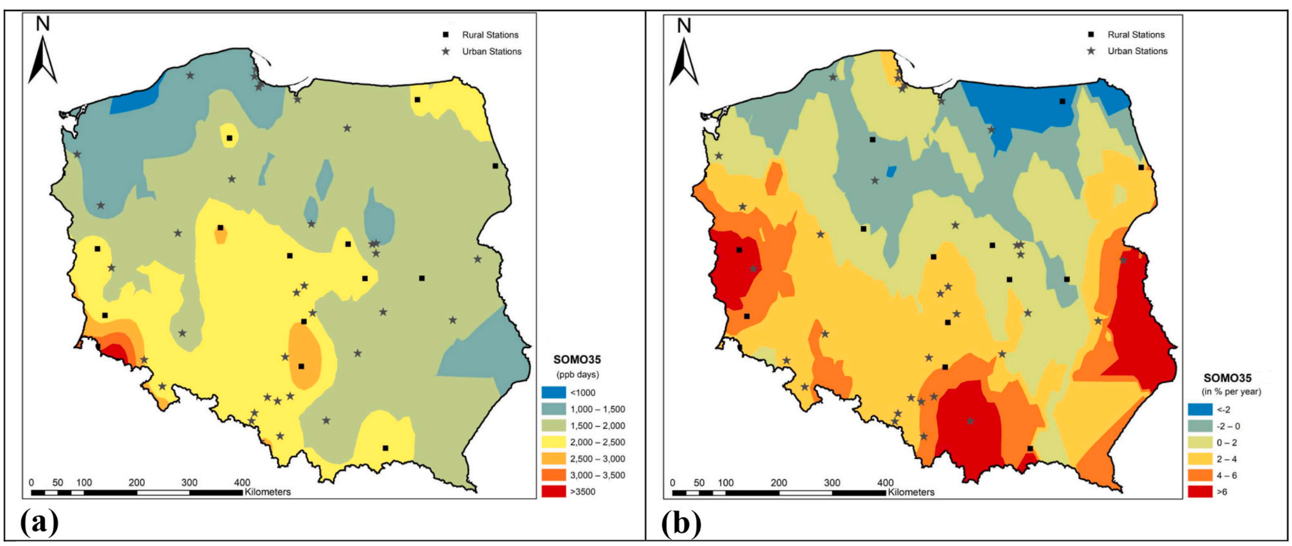

Fig. 4. Annual SOMO35 values (a) and annual trend magnitude (b) calculated by joining annual data from 16 rural and 36 urban stations over the time period 2010–2019.

hourly maxima ranged from - 1.42% $year^{-1}$ in Jarczew (east) to + 2.80% $year^{-1}$ in Smolary Bytnickie (west). At urban sites, the trends ranged from - 2.22% $year^{-1}$ in Zabrze (south) to + 2.34% $year^{-1}$ in Radom (central region).

Regarding human health, the trends in SOMO35, summertime O_3 MDA8, and EU60 mean values are presented in Figs. 4b, 5b and 6b, respectively. High declines in SOMO35 (less than - 2.0% $year^{-1}$), summertime O_3 MDA8 (less than - 1.0% $year^{-1}$) and EU60 (less than - 1 days $year^{-1}$) were observed in northeastern Poland while significant increases in SOMO35 (more than + 6.0% $year^{-1}$), summertime O_3 MDA8 (more than + 1.5% $year^{-1}$) and EU60 (more than + 2 days $year^{-1}$) were found in southeast and western Poland. In rural areas, the trends in SOMO35 ranged from - 4.31% $year^{-1}$ in Jarczew (east) to + 11.45% $year^{-1}$ in Smolary Bytnickie (west), summertime O_3 MDA8 ranged from - 1.30% $year^{-1}$ in Puszcza (north) to + 1.51% $year^{-1}$ in Widuchowa (west), and EU60 ranged from - 3.3 days per year in Śnieżka (southwest) to + 2.7 days per year in Smolary Bytnickie (west). In urban areas, SOMO35 varied from - 3.07% $year^{-1}$ in Gdansk (north) to + 17.36% $year^{-1}$ in Kraków (southeast), summertime O_3 MDA8 ranged from - 0.68% $year^{-1}$ in Olsztyn (northeastern) to + 2.30% $year^{-1}$ in in Kraków (southeast), and the trends in EU60 ranged from - 2.42 days per year in Cieszyn (south) to + 1.25 days per year in Dabrowa Górnicza (south).

The spatial distribution of trends in vegetation impact metrics are similar between AOT40c (Fig. 7b) and AOT40f (Fig. 8b) with higher increases (more than + 8.0% $year^{-1}$) observed in southeast and western Poland, and higher declines (less than - 2.0% $year^{-1}$) found in northern Poland. In rural areas, the trends in AOT40c and AOT40f ranged from - 5.01% $year^{-1}$ and - 3.83% $year^{-1}$ in Jarczew (east) to + 16.20% $year^{-1}$ and +22.35% $year^{-1}$ in Smolary Bytnickie (west). In urban areas, the trends in AOT40c ranged from - 4.34% $year^{-1}$ in Elblag (north) to + 34.10% $year^{-1}$ in Kraków (southeast), while trends in AOT40f in urban areas ranged from - 2.75% in Gdansk (north) to + 38.09% in Kraków (southeast).

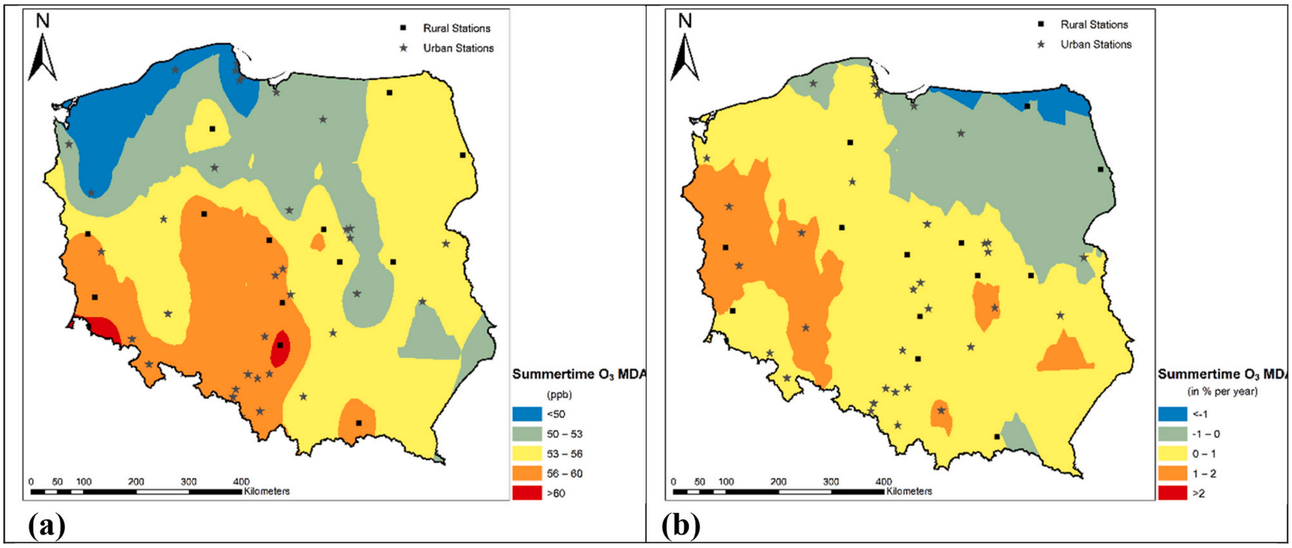

Fig. 5. The highest seasonal average daily 8-h maximum ozone concentration, abbreviated as "summertime O_3 MDA8" (a) and annual trend magnitude (b) calculated by joining annual data from 16 rural and 36 urban stations over the time period 2010–2019.

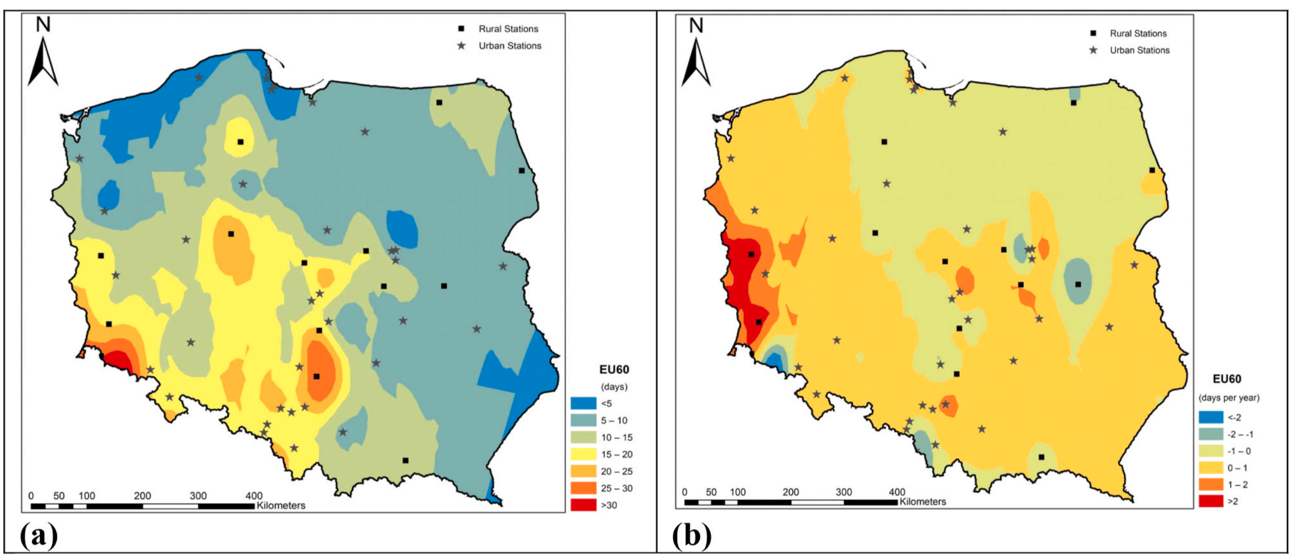

Fig. 6. EU60, number of daily maximum 8-h means over 60 ppb (a) and annual trend magnitude (b) calculated by joining annual data from 16 rural and 36 urban stations over the time period 2010–2019.

4. Discussion

4.1. Spatial distribution of ground-level ozone metrics

Surface O_3 mean concentrations vary significantly over space and time (e.g., Sicard et al., 2017; Boleti et al., 2020; De Marco et al., 2022). Hence, the generation of spatiotemporal maps of O_3 metrics is crucial for accurate risk assessment (Lefohn et al., 2018; De Marco et al., 2022) and can provide valuable information on the spatial distribution of areas at high and medium O_3 risk (Downey et al., 2015; Paoletti et al., 2019; De Marco et al., 2022). In this study, a kriging interpolation method, suitable for spatial mapping of ground-based observations of O_3 (Sicard et al., 2016a), has been applied to overcome the lack of monitoring stations in some areas and allowed the creation of a continuous information layer.

The highest annual O_3 mean concentrations and 50th percentiles (>30 ppb) were recorded in southwestern Poland, while the lowest annual O_3 levels (<20 ppb) and highest hourly maxima (>90 ppb) were observed in major cities and downwind of industrial areas nearby Kraków, Katowice, and Warsaw with high NO_x and VOCs emissions (Bebkiewicz et al., 2020). In urban areas, fresh nitrogen oxides (NO) emissions from road traffic, can deplete O_3 locally (Sicard et al., 2020a; Agathokleous S. et al., 2022; Calatayud et al., 2023). Higher annual O_3 mean concentrations were recorded in rural areas (on average, 28 ppb), mainly due to higher emissions of biogenic VOCs, weakened O_3 titration by NO, and transport of O_3 and precursors from major urban centers (Monks et al., 2015; Sicard et al., 2016a). Higher O_3 levels (on average, 40 ppb) at mountainous areas than lowland areas can be explained by higher solar radiation, biogenic VOCs emissions, and stratospheric O_3 inputs into the troposphere (e.g., Chevalier et al., 2007; Lefohn et al., 2012; Sicard et al., 2016a) as well as by reduced O_3 uptake by plants due to different conditions of light, air temperature, and vapor pressure deficit controlling the O_3 deposition at high-elevation sites (Turnipseed et al., 2009). In Cyprus, Agathokleous S. et al. (2022) also recorded the highest O_3 levels at the mountainous station Mt. Troodos (~1800 m a.s.l). The annual O_3 mean concentrations recorded in Poland are like those

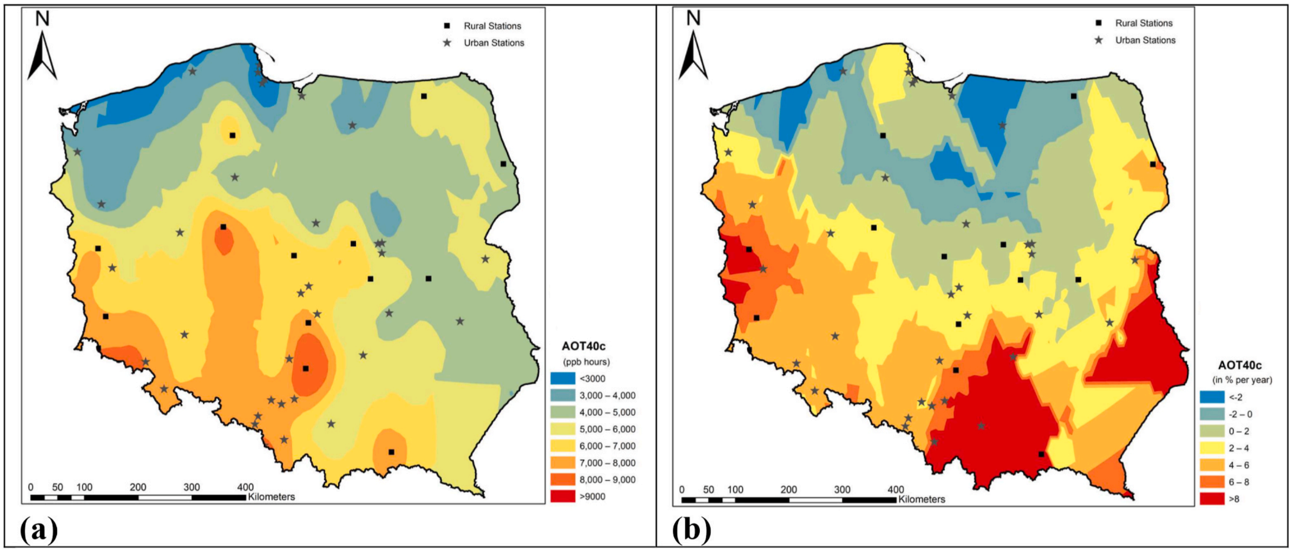

Fig. 7. AOT40c, i.e., sum of the hourly concentrations above 40 ppb during the growing season for crops (a) and annual trend magnitude (b) calculated by joining annual data from 16 rural and 36 urban stations over the time period 2010–2019.

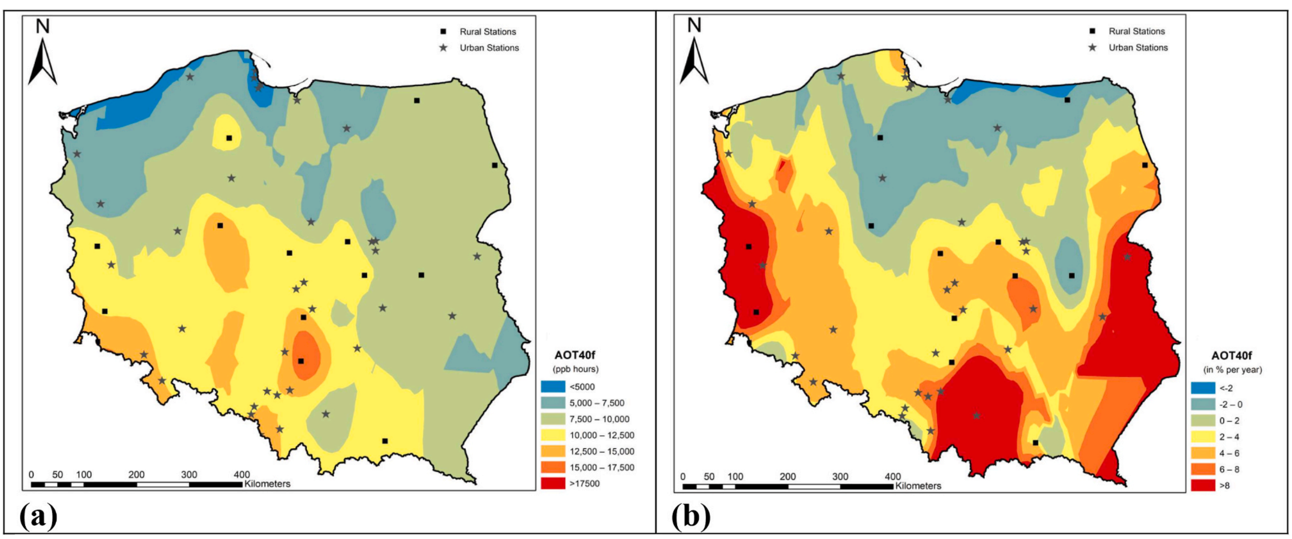

Fig. 8. AOT40f, i.e., sum of the hourly concentrations above 40 ppb during the growing season for forests (a) and annual trend magnitude (b) calculated by joining annual data from 16 rural and 36 urban stations over the time period 2010–2019.

observed across Europe (e.g., Sicard et al., 2013, 2016a), but lower than O_3 levels observed in the United States and Japan (Sicard et al., 2020a).

Elevated O_3 exposures are harmful for human health, vegetation, and agricultural crops (Mills et al., 2018; De Marco et al., 2022; Eghdami et al., 2022; Sicard et al., 2023), and current ambient levels are high enough to adversely affect vegetation (e.g., Paoletti et al., 2019; Sicard et al., 2020a; Proietti et al., 2021; Anav et al., 2022) and human health (Malashock et al., 2022) in central Europe. In Polish cities, the annual number of premature deaths attributed to surface O_3 increased by 0.45 deaths per 10^6 inhabitants over 2000–2017 (Sicard et al., 2021b). To evaluate the effects of exposure and guide agendas addressing human health and vegetation protection, exposure-based metrics such as AOT40, SOMO35, summertime O_3 MDA8, and EU60 were established (Lefohn et al., 2018). Such metrics are a reliable and informative approach to verify the efficiency of the control strategies for reducing the surface O_3 levels and for mitigating the adverse effects on human health and vegetation (Monks et al., 2015). In Poland, the lowest SOMO35, summertime O_3 MDA8, and EU60 values were recorded in cities, while the highest values were found in rural areas. For both human health exposure metrics, a strong gradient southwest-to-northwest occurred across Poland, with the highest O_3 human health metrics (SOMO35 $>$ 3000 ppb days, summertime O_3 MDA8 $>$ 55 ppb, and EU60 $>$ 25 days per year) observed in southwestern Poland, particularly in industrialized and urbanized areas (central Poland) and mountains areas (southwestern Poland) where the critical levels are regularly exceeded. In Slovakia, the SOMO35 values at 27 monitoring stations ranged from 880 to 9500 ppb days over 2001–2005 (Kremler, 2007). For O_3 impact assessment on vegetation, the concentration-based AOT40 exposure index has been used. Higher AOT40c and AOT40f values were recorded at rural stations (on average, ~6900 and 12,200 ppb h, respectively) than at urban stations (on average, ~5400 and 9200 ppb h, respectively). Over the time period 2010–2019, the gradient of the AOT40c values was similar to AOT40f, i.e., lower AOT40c (<3000 ppb h) and AOT40f (<5000 ppb h) in northwestern Poland and higher values (AOT40c > 7000 ppb h; AOT40f > 12, 000 ppb h) found in rural areas at mountainous station in southwestern

Poland and downwind of urbanized areas in southern and central. In Slovakia, the mean exposures for forests range between 8500 and 28, 300 ppb h and between 5300 and 16,900 ppb h for crops over 2001–2005 (Kremler, 2007).

4.2. Short-term trends of ozone metrics

The annual O_3 mean concentrations and 50th percentiles increased in southern Poland and declined in northern Poland with a clear Southeastern-North gradient. In northern Poland, all O_3 metrics declined over the study period. The hourly maxima and human health and vegetation exposure metrics increased in western and southeastern Poland, while EU60 declined in southeastern Poland, nearby Kraków and surroundings cities. In urban areas, the annual O_3 mean concentrations and 50th percentiles increased by 0.81% year^{-1} and 1.06% year^{-1}, respectively, over 2010–2019. An increase of annual O_3 mean concentrations was observed at 75% of urban stations. A slight decline of the number of O_3 peaks occurred at urban stations, i.e., hourly maxima (- 0.10% year^{-1}), while we obtained significant increase (>3% per year) for SOMO35, AOT40c, and AOT40f, and a slight increase for EU60 and summertime O_3 MDA8. In rural areas, the trend in 50th percentiles is relatively null, while annual O_3 mean concentrations are rising (+0.12% year^{-1}) at 62.5% of rural stations, i.e., that the O_3 peaks and hourly maxima (+0.23% year^{-1}) increased. The human health and vegetation impact metrics also increased over the study period.

In Poland, the NO_x and NMVOCs emissions mainly result from energy industries (68% and 25%) and road transport (29% and 11%). The consumption of coal for residential heating is still relatively high compared to neighboring Germany and the Czech Republic, and energy is mostly obtained from coal burning (Bebkiewicz et al., 2020). Between 1990 and 2017, the annual emissions from road transport have increased for NO_x (+25%), mainly due to the increase in the transport activity, while a decrease of NMVOCs (- 85%) has been reported (Bebkiewicz et al., 2020). From 2017, with the latest Euro quality standards for vehicles, the NO_x emissions are declining. The largest reduction of NMVOCs occurred in road transport and from coal mining and handling (Bebkiewicz et al., 2020). In Poland, the control strategies to reduce emissions over 2010–2019 focused more on NO_x than on VOCs (- 2.33 and - 0.95% per year, respectively), therefore most areas are under VOCs-limited conditions with a predominant role of reduced O_3 titration by NO (Akimoto and Tanimoto, 2022; Zhang et al., 2022).

A deep review of surface O_3 trends at urban and rural stations worldwide has been published (Sicard, 2021). Since the 2000s, most studies have reported an upward trend for annual O_3 mean concentrations in urban areas worldwide (Sicard, 2021). For instance, between 2005 and 2014, the background O_3 levels have increased more in Japan, Spain, and France than in Poland, and less in Germany and the United States over 2005–2018 (Table 3). In France, significant increases of O_3 mean concentrations and 50th percentiles (~0.6% year^{-1}) were reported at urban stations, while exposure metrics declined (~- 1.0–2.0% year^{-1}) between 1999 and 2012 (Sicard et al., 2016a). Between 2010 and 2019, the trends in summertime O_3 MDA8 ranged between −1 and +1% year^{-1} in urban areas with more 50,000 inhabitants in Central and Southern Europe (Sicard et al., 2023). The upward trend of O_3 observed in most urban areas worldwide (under VOC-limited photochemical regime) can be attributed to a weakened O_3 titration due to lower NO_x emissions from e.g., road transport (Simpson et al., 2014; Sicard, 2021; Ren and Xie, 2022). Since the 1990s, the emission control strategies established by national governments focused more on NO_x than on VOCs emissions, leading to enhanced O_3 concentrations in cities (Lefohn et al., 2018; Sicard et al., 2021b). The vehicle emission regulations could explain the slight reduction in O_3 peaks at urban stations (de Foy et al., 2020). Conversely, most studies have reported significant declines of annual O_3 mean concentrations in rural areas worldwide (Sicard, 2021), for instance, in Germany and the United States over 2005–2018 (Table 3). From 2000s, the human health and vegetation impact metrics decreased in most European rural areas (e.g., Sicard et al., 2016a; Chang et al., 2017). However, like in Poland the O_3 levels rose (>+ 0.5% year^{-1}) in rural areas in The Netherlands and Slovakia between 2005 and 2014 (Sicard et al., 2020a), and in East Asia between 2000 and 2014 (Chang et al., 2017). The increase in background O_3 levels (and low percentiles) in rural areas can be attributed to i) long-range transport of O_3 and its precursors (Lefohn and Cooper, 2015; Malley et al., 2015), e.g., from Russia where the NO_x and VOCs emissions increased in 2010–2019, ii) climate change (Sicard et al., 2017; Traczyk and Gruszecka-Kosowska, 2020), and iii) a weakened titration of O_3 by NO at regional scale (Sicard et al., 2017).

By using multi-scale models, Szopa and Hauglustaine (2007) evaluated the potential changes in human health exposure (SOMO35) in Europe by 2030 and showed that Poland is among the countries exhibiting an increase in surface O_3 levels. The trends in exposure metrics (AOT40 and SOMO35) are influenced by changes in background O_3 levels and by local NO_x emissions, particularly in urban areas (Malley et al., 2015), while summertime O_3 MDA8 and EU60 trends are mainly influenced by O_3 peaks (Tørseth et al., 2012). For all O_3 metrics, the greatest increases were observed at locations with the largest NO_x and VOCs emissions e.g., industrialized areas in Southeastern Poland such as Katowice, Kraków, and surroundings cities where poor-quality coal stoves are still widely used for residential heating. Since September 2019, burning of solid fuels (coal and wood) in boilers, stoves or fireplaces is prohibited in the city of Kraków (Traczyk and Gruszecka-Kosowska, 2020). In areas under a NO_x-limited photochemical regime, an increase in NO_x levels leads to O_3 formation, while an increase in VOCs has a small effect on O_3 burden (Markakis et al., 2014; McDonald et al., 2018; Akimoto and Tanimoto, 2022). Anav et al. (2019) have observed an increase in NO_x levels in southern and central Poland over 2001–2014.

Due to missing meteorological data from ground stations or meteorological models (De Marco et al., 2022), we did not explore the relationships between O_3 precursors, meteorological parameters, and surface O_3 levels. Climate change (e.g., rising air temperature) is projected to reduce the benefits of O_3 precursor emissions controls (Colette et al., 2015; Sicard and Dalstein-Richier, 2015). By 2100, future climate scenarios present a penalty for ground-level O_3 of about 5 ppb in summer across Europe (Colette et al., 2015). Climate change creates additional challenges for population health and well-being (Kjellstrom and McMichael, 2013), forest management (Sicard and Dalstein-Richier, 2015) and biological diversity (Agathokleous et al., 2020).

5. Conclusions

Based on a ten-year pre-COVID19 analysis (2010–2019) in Poland, people living in rural areas are exposed to higher O_3 levels compared to those living in cities (e.g., SOMO35 = 2440 vs. 1760 ppb days). Southeastern Poland, where coal stoves are still the dominant heating system, is at high O_3 risk. The O_3 baseline level is rising in the Polish cities and rural areas despite the recent reduction of NO_x and VOCs emissions. In cities, rising annual O_3 mean concentrations and the slight reduction in O_3 peaks are likely driven by the recent reductions in NO_x emissions by vehicles (Euro quality standards). The increase in background O_3 levels in rural areas can be attributed to long-range transport of O_3 and its precursors, to climate change, and a weakened O_3 titration by NO_x emissions decline at regional scale. Risks of O_3 exposure for human health and vegetation were documented, and the increase is likely driven by higher photochemical O_3 formation at regional scale and rising background O_3 levels, in particular in summer.

A major concern is related to the upward trends and overrun of exposure metrics compared to the target values and critical levels for human health and vegetation protection. Despite that O_3 precursor emissions declined, human health and vegetation are threatened by O_3, in particular in Southern Poland. In Poland, 1500 premature deaths are attributed to ambient O_3 exposure in 2018 (EEA, 2020). Both human health exposure metrics (SOMO35, summertime O_3 MDA8, and EU60) do not take into account the harmful effects of rising O_3 baseline levels on human health over time. Linearity and the presence of a threshold, below which O_3 does not adversely affect mortality, is controversial (Nasari et al., 2016). Bae et al. (2015) have reported non-linear concentration-response relationship with thresholds (30-40 ppb) between daily O_3 mean concentration and daily number of non-accidental deaths in Japanese and Korean cities from 2000 to 2009. Bell et al. (2006) showed that even low O_3 concentrations (<15 ppb), below the WHO regulations, are associated with increased risk of all-cause premature mortality. A "safe" daily O_3 level would be lower than 10 ppb (Bell et al., 2006). To protect population against O_3, the use of non-linear metrics with no exposure threshold could be recommended.

The exposure-based index (AOT40) appears unsuitable for the vegetation protection against O_3 pollution (De Marco et al., 2015; Paoletti et al., 2019; Sicard et al., 2020b). In the last decades, the assessments of O_3 effects on plants have incorporated metrics with relatively high cut-offs of concentration levels (e.g., hourly 40 ppb) while stress biology commonly follows non-linear responses (Conte et al., 2021) and relatively low concentrations can reduce subsequent damage via hormetic preconditioning mechanisms or even lead to more negative effects in the long term (Agathokleous et al., 2019). Ozone effects on vegetation depend not only on the O_3 concentrations in the air but also on O_3 uptake through the stomata (Paoletti et al., 2022). Therefore, a stomatal flux-based metric, i.e., the Phytotoxic Ozone Dose with Y the O_3 detoxification threshold (PODY), has been introduced for vegetation protection against effects of O_3 (Sicard et al., 2016b). The tolerance to O_3 changes seasonally ("dynamic threshold") with higher tolerance in winter and spring and lower thresholds in summer and fall (Conte et al., 2021). Sicard et al. (2016b) have recommended the use of POD0, calculated over the 24-h exposure period of time during the growing season, for vegetation risk assessment. For more realistic assessments, new metrics are needed with no (or lower) concentration cut-offs, and by taking into account plant defense mechanisms (Wu et al., 2021). However, their real-world regulatory application is technically highly difficult due to the high needs of data and the requirement of instruments, skills, and trained personnel.

The local O_3 formation depends on the VOCs-to-NO_x ratio (Huszar et al., 2015). In urban areas, to efficiently mitigate O_3 pollution, we recommend to significantly reduce VOCs sources in addition to reductions of NO_x emissions (Huszar et al., 2015; McDonald et al., 2018). By selecting plant species that are low VOC emitters, urban vegetation, in particular urban trees (Sicard et al., 2018), can effectively reduce rising O_3 concentrations in Polish cities as demonstrated in different urban contexts (Florence, Italy; Bucharest, Romania; Tokyo, Japan) with different meteorological and pollution conditions (Sicard et al., 2022; Manzini et al., 2023).

Author contributions

AC, EQ, and PS have contributed to the study conception and design. Data collection and analysis were performed by AC, FC, SL, and EQ. The first draft of the manuscript was written by AC and PS. ADM, SL, and EA have commented and revised the manuscript. All authors read and approved the final manuscript.

Declaration of competing interest

The authors declare that they have no known competing financial interests or personal relationships that could have appeared to influence the work reported in this paper.

Data availability

Data will be made available on request.

Acknowledgements

This work was made possible by using the data from the air quality database AirBase (European Environment Agency) in the framework of the Working Party 8.04.05 "Ground-level ozone" under the Research Group 8.04.00 "*Air Pollution and Climate Change*" of the International Union of Forest Research Organizations. This work was carried out with the contribution of the LIFE financial instrument of the European Union in the framework of the AIRFRESH project "*Air pollution removal by urban forests for a better human well-being*" (LIFE19 ENV/FR/000086).

Appendix A. Supplementary data

Supplementary data to this article can be found online at https://doi.org/10.1016/j.atmosenv.2023.119926.

References

Adame, J.A., et al., 2022. Surface ozone trends over a 21-year period at el arenosillo observatory (southwestern Europe). Atmos. Res. 269, 106048.
Agathokleous, E., Feng, Z., Peñuelas, J., 2022. Ozone pollution disrupts plant-pollinator systems. Trends Ecol. Evol. 37 (11), 939–941.
Agathokleous, S., Saitanis, C.J., Savvides, C., Sicard, P., Agathokleous, E., et al., 2022. Spatio-temporal variation of ozone exposure and its risks to vegetation and human health in Cyprus: an analysis across a gradient of altitudes. J. For. Res. https://doi.org/10.1007/s11676-022-01520-2.
Agathokleous, E., Feng, Z., Oksanen, E., Sicard, P., Wang, Q., et al., 2020. Ozone affects plant, insect, and soil microbial communities: a threat to terrestrial ecosystems and biodiversity. Sci. Adv. 6, eabc1176.
Agathokleous, E., Araminiene, V., Belz, R., Calatayud, V., De Marco, A., et al., 2019. A quantitative assessment of hormetic responses of plants to ozone. Environ. Res. 176, 108527.
Akimoto, H., Tanimoto, H., 2022. Rethinking of the adverse effects of NOx-control on the reduction of methane and tropospheric ozone – challenges toward a denitrified society. Atmos. Environ. 277, 119033.
Anav, A., De Marco, A., Collalti, A., Emberson, L., Feng, Z., et al., 2022. Legislative and functional aspects of different metrics used for ozone risk assessment to forests. Environ. Pollut. 295, 118690.
Anav, A., De Marco, A., Friedlingstein, P., Khvorostyanov, D., Menut, L., et al., 2019. Growing season extension affects ozone uptake by European forests. Sci. Total Environ. 669, 1043–1052.
Araminienė, V., Sicard, P., Anav, A., Agathokleous, E., Stakėnas, V., De Marco, A., Varnagirytė-Kabašinskienė, I., Paoletti, E., Girgždienė, R., 2019. Trends and inter-relationships of ground-level ozone metrics and forest health in Lithuania. Sci. Total Environ. 658, 1265–1277.
Bae, S., Lim, Y.H., Kashima, S., Yorifuji, T., Honda, Y., et al., 2015. Non-linear concentration-response relationships between ambient ozone and daily mortality. PLoS One 10 (6), e0129423.
Bebkiewicz, K., Chłopek, Z., Lasocki, J., Szczepański, K., Zimakowska-Laskowska, M., 2020. The inventory of pollutants hazardous to the health of living organisms, emitted by road transport in Poland between 1990 and 2017. Sustainability 12, 5387.
Bell, M.L., Peng, R.D., Dominici, F., 2006. The exposure–response curve for ozone and risk of mortality and the adequacy of current ozone regulations. Environ. Health Perspect. 114, 532–536.
Boleti, E., Hueglin, C., Grange, S.K., Prévôt, A.S.H., Takahama, S., 2020. Temporal and spatial analysis of ozone concentrations in Europe based on time scale decomposition and a multi-clustering approach. Atmos. Chem. Phys. 20, 9051–9066.
Calatayud, V., Diéguez, J.J., Agathokleous, E., Sicard, P., 2023. Machine Learning Model to Predict Vehicle Electrification Impacts on Urban Air Quality and Related Human Health Effects.". Environmental Research, 115835.
Chang, K.L., Petropavlovskikh, I., Cooper, O.R., Schultz, M.G., Wang, T., 2017. Regional trend analysis of surface ozone observations from monitoring networks in eastern North America, Europe and East Asia. Elementa: Science of the Anthropocene 5, 50.
Chattopadhyay, G., Chakraborthy, P., Chattopadhyay, S., 2012. Mann–Kendall trend analysis of tropospheric ozone and its modeling using ARIMA. Theor. Appl. Climatol. 110, 321–328.
Chevalier, A., Gheusi, F., Delmas, R., Ordonez, C., Sarrat, C., et al., 2007. Influence of altitude on ozone levels and variability in the lower troposphere: a ground-based study for western Europe over the period 2001-2004. Atmos. Chem. Phys. 7, 4311–4326.
Cohen, A.J., Brauer, M., Burnett, R., Anderson, H.R., Frostad, J., et al., 2017. Estimates and 25-year trends of the global burden of disease attributable to ambient air pollution: an analysis of data from the Global Burden of Diseases Study 2015. Lancet 389, 1907–1918.
Colette, A., Andersson, C., Baklanov, A., Bessagnet, B., Brandt, J., et al., 2015. Is the ozone climate penalty robust in Europe? Environ. Res. Lett. 10, 084015.
Conte, A., Otu-Larbi, F., Alivernini, A., Hoshika, Y., Paoletti, P., et al., 2021. Exploring new strategies for ozone-risk assessment: a dynamic-threshold case study. Environ. Pollut. 287, 117620.

de Foy, B., Brune, W.H., Schauer, J.J., 2020. Changes in ozone photochemical regime in Fresno, California from 1994 to 2018 deduced from changes in the weekend effect. Environ. Pollut. 263, 114380.
De Leeuw, F., 2000. Trends in ground level ozone concentrations in the European Union. Environ. Sci. Pol. 3, 189–199.
De Marco, A., Garcia-Gomez, H., Collalti, A., Khaniabadi, Y.O., Feng, Z., Proietti, C., Sicard, P., Vitale, M., Anav, A., Paoletti, E., 2022. Ozone modelling and mapping for risk assessment: an overview of different approaches for human and ecosystems health. Environ. Res. 211, 113048.
De Marco, A., Sicard, P., Vitale, M., Carriero, G., Renou, C., et al., 2015. Metrics of ozone risk assessment for Southern European forests: canopy moisture content as a potential plant response indicator. Atmos. Environ. 120, 182–190.
Downey, N., Emery, C., Jung, J., Sakulyanontvittaya, T., Hebert, L., Doug Blewitt, D., Greg Yarwood, G., 2015. Emission reductions and urban ozone responses under more stringent US standards. Atmos. Environ. 101, 209–216.
EC, European Commission, 2008. Directive 2008/50/EC of the European Parliament and of the Council of 21 May 2008 on ambient air quality and cleaner air for Europe. Official Journal L 152, 1–44, 11.6.2008.
EC, European Commission, 2002. Directive 2002/3/EC of the European Parliament and of the Council of 12 February 2002 relating to ozone in ambient air. Official Journal L 67/14, 1–23, 9.3.2002.
EC, European Commission, 1992. Council Directive 92/72/EEC of 21 September 1992 on air pollution by ozone. Official Journal L 297, 1–7, 13.10.1992.
European Environment Agency, 2020. European Union Emission Inventory Report 1990-2020 under the UNECE Air Convention. EEA Report No 03/2022.
Eghdami, H., Werner, W., Büker, P., Sicard, P., 2022. Assessment of ozone risk to Central European forests: time series indicates perennial exceedance of ozone critical levels. Environ. Res. 203, 111798.
Ellingsen, K., Gauss, M., Van Dingenen, R., Dentener, F.J., Emberson, L., et al., 2008. Global ozone and air quality: a multi-model assessment of risks to human health and crops. Atmos. Chem. Phys. Discuss. 8, 2163–2223.
Emberson, L., 2020. Effects of ozone on agriculture, forests and grasslands. Phil. Trans. R. Soc. A378, 20190327.
Fleming, Z.L., Doherty, R.M., von Schneidemesser, E., Malley, C.S., Cooper, O.R., et al., 2018. Tropospheric Ozone Assessment Report: present-day ozone distribution and trends relevant to human health. Elem Sci Anth 6, 12.
GBD, Global Burden of Disease, 2020. Global burden of 369 diseases and injuries in 204 countries and territories, 1990-2019: a systematic analysis for the Global Burden of Disease Study 2019. Lancet 396 (2020), 1204–1222.
Guerreiro, C.B.B., Foltescu, V., de Leeuw, F., 2014. Air quality status and trends in Europe. Atmos. Environ. 98, 376–384.
Huszar, P., Belda, M., Halenka, T., 2015. On the long term impact of emissions from central European cities on regional air-quality. Atmos. Chem. Phys. Discuss. 15, 32101–32155.
IPCC, Intergovernmental Panel on Climate Change, 2022. In: Pörtner, H.-O., Roberts, D. C., Tignor, M., Poloczanska, E.S., Mintenbeck, K., Alegría, A., Craig, M., Langsdorf, S., Löschke, S., Möller, V., Okem, A., Rama, B. (Eds.), Climate Change 2022: Impacts, Adaptation and Vulnerability." Contribution of Working Group II to the Sixth Assessment Report of the Intergovernmental Panel on Climate Change. Cambridge University Press, Cambridge, UK and New York, NY, USA, p. 3056. Cambridge University Press.
Javanmardi, P., Morovati, P., Farhadi, M., Geravandi, S., Khaniabadi, Y.O., et al., 2018. Monitoring the impact of ambient ozone on human health using time series analysis and air quality model approaches. Fresenius Environ. Bull. 26, 533–544.
Kjellstrom, T., McMichael, A.J., 2013. Climate change threats to population health and well-being: the imperative of protective solutions that will last. Glob. Health Action 6, 20816.
Kracht, O., Santiago, J.L., Martin, F., Piersanti, A., Cremona, G., et al., 2017. Spatial Representativeness of Air Quality Monitoring Sites - Outcomes of the FAIRMODE/AQUILA Intercomparison Exercise.". Publications Office of the European Union, Luxembourg, 2017, ISBN 978-92-79-77218-4, JRC108791.
Kremler, M., 2007. Ozone exposure indices in Slovakia. In: Proceeding, International Scientific Conference, Poľana Nad Detvou, Slovakia. September 17 - 20, 2007.
Lefohn, A.S., Malley, C.S., Smith, L., Wells, B., Hazucha, M., Simon, H., et al., 2018. Tropospheric ozone assessment report: global ozone metrics for climate change, human health, and crop/ecosystem research. Elementa: Science of the Anthropocene 6, 28.
Lefohn, A.S., Cooper, O.R., 2015. Introduction to the special issue on observations and source attribution of ozone in rural regions of the western United States. Atmos. Environ. 109, 279–281.
Lefohn, A.S., Wernli, H., Shadwick, D., Oltmans, S.J., Shapiro, M., 2012. Quantifying the frequency of stratospheric-tropospheric transport affecting enhanced surface ozone concentrations at high- and low-elevation monitoring sites in the United States. Atmos. Environ. 62, 646–656.
Malashock, D.A., Delang, M.N., Becker, J.S., Serre, M.L., West, J.J., et al., 2022. Estimates of ozone concentrations and attributable mortality in urban, peri-urban and rural areas worldwide in 2019. Environ. Res. Lett. 17, 054023.
Malley, C.S., Heal, M.R., Mills, G., Braban, C.F., 2015. Trends and drivers of ozone human health and vegetation impact metrics from UK EMEP supersite measurements (1990-2013). Atmos. Chem. Phys. 15, 4025–4042.
Manzini, J., Hoshika, Y., Carrari, E., Sicard, P., Watanabe, M., et al., 2023. FlorTree: a unifying modelling framework for estimating the species-specific pollution removal by individual trees and shrubs. Urban For. Urban Green. 85, 127967.
Markakis, K., Valari, M., Colette, A., Sanchez, O., Perrussel, O., et al., 2014. Air-quality in the mid-22St century for the city of Paris under two climate scenarios; from regional to local scale. Atmos. Chem. Phys. 14, 95–136.
McDonald, B.C., de Gouw, J.A., Gilman, J.B., Jathar, S.H., Akherati, A., et al., 2018. Volatile chemical products emerging as largest petrochemical source of urban organic emissions. Science 359 (6377), 760–764.
Mills, G., Pleijel, H., Malley, C.S., Sinha, B., Cooper, O.R., et al., 2018. Tropospheric Ozone Assessment Report: present-day tropospheric ozone distribution and trends relevant to vegetation. Elementa: Science of the Anthropocene 6, 47.
Monks, P.S., Archibald, A.T., Colette, A., Cooper, O., Coyle, M., et al., 2015. Tropospheric ozone and its precursors from the urban to the global scale from air quality to short-lived climate forcer. Atmos. Chem. Phys. 15, 8889–8973.
Nasari, M.M., Szyszkowicz, M., Chen, H., Crouse, D., Turner, M.C., et al., 2016. A class of non-linear exposure-response models suitable for health impact assessment applicable to large cohort studies of ambient air pollution. Air Qual. Atmos. Health 9, 961–972.
Nuvolone, D., Petri, D., Voller, F., 2018. The effects of ozone on human health. Environ. Sci. Pollut. Res. 25, 8074–8088.
Paoletti, E., Sicard, P., Hoshika, Y., Fares, S., Badea, O., et al., 2022. Towards long-term sustainability of stomatal ozone flux monitoring at forest sites. Sustainable Horizons 2, 100018.
Paoletti, E., Alivernini, A., Anav, A., Badea, O., Chivulescu, S., et al., 2019. Toward stomatal–flux based forest protection against ozone: the MOTTLES approach. Sci. Total Environ. 691, 516–527.
Proietti, C., Fornasier, M.F., Sicard, P., Anav, A., Paoletti, E., et al., 2021. Trends in tropospheric ozone concentrations and forest impact metrics in Europe over the time period 2000-2014. J. For. Res. 31, 1–9.
Ren, J., Xie, S., 2022. Diagnosing ozone-NOx-VOC sensitivity and revealing causes of ozone increases in China based on 2013-2021 satellite retrievals. Atmos. Chem. Phys. 22, 15035–15047.
Schultz, M.G., Schröder, S., Lyapina, O., Cooper, O., Galbally, I., et al., 2017. Tropospheric Ozone Assessment Report: database and metrics data of global surface ozone observations. Elem. Sci. Anth. 5, 58.
Screpanti, A., De Marco, A., 2009. Corrosion on cultural heritage buildings in Italy: a role for ozone? Environ. Pollut. 157, 1513–1520.
Sicard, P., Agathokleous, E., Anenberg, S.C., De Marco, A., Paoletti, E., et al., 2023. Trends in urban air pollution over the last two decades: a global perspective. Sci. Total Environ. 858, 160064.
Sicard, P., Agathokleous, E., Araminiene, V., Carrari, E., Hoshika, Y., et al., 2018. Should we see urban trees as effective solutions to reduce increasing ozone levels in cities? Environ. Pollut. 243, 163–17.
Sicard, P., Agathokleous, E., De Marco, A., Paoletti, E., 2022. Ozone-reducing urban plants: choose carefully. Science 377 (6606), 585, 585.
Sicard, P., Hoshika, Y., Carrari, E., De Marco, A., Elena, P., 2021a. Testing visible ozone injury within a Light Exposed Sampling Site as a proxy for ozone risk assessment for European forests. J. For. Res. 32, 1351–1359.
Sicard, P., Agathokleous, E., De Marco, A., Paoletti, E., Calatayud, V., 2021b. Urban population exposure to air pollution in Europe over the last decades. Environ. Sci. Eur. 33, 28.
Sicard, P., 2021. Ground-level ozone over time: an observation-based global overview. Current Opinion in Environmental Science & Health 19, 100226.
Sicard, P., Paoletti, E., Agathokleous, E., Araminienė, V., Proietti, C., et al., 2020a. Ozone weekend effect in cities: deep insights for urban air pollution control. Environ. Res. 191, 110193.
Sicard, P., De Marco, A., Carrari, E., Dalstein-Richier, L., Hoshika, Y., et al., 2020b. Epidemiological derivation of flux-based critical levels for visible ozone injury in European forests. J. For. Res. 31, 1509–1519.
Sicard, P., Anav, A., De Marco, A., Paoletti, E., 2017. Projected global ground-level ozone impacts on vegetation under different emission and climate scenarios. Atmos. Chem. Phys. 17, 12177–12196.
Sicard, P., Serra, R., Rossello, P., 2016a. Spatio-temporal trends of surface ozone concentrations and metrics in France. Environ. Res. 149, 122–144.
Sicard, P., De Marco, A., Dalstein-Richier, L., Tagliaferro, F., Paoletti, E., 2016b. An epidemiological assessment of stomatal ozone flux-based critical levels for visible ozone injury in Southern European forests. Sci. Total Environ. 541, 729–741.
Sicard, P., Dalstein-Richier, L., 2015. Health and vitality assessment of two common pine species in the context of climate change in Southern Europe. Environ. Res. 137, 235–245.
Sicard, P., De Marco, A., Troussier, F., Renou, C., Vas, N., et al., 2013. Decrease in surface ozone concentrations at Mediterranean remote sites and increase in the cities. Atmos. Environ. 79, 705–715.
Simpson, D., Arneth, A., Mills, G., Solberg, S., Uddling, J., 2014. Ozone - the persistent menace: interactions with the N cycle and climate change. Curr. Opin. Environ. Sustain. 9–10, 9–19.
Snel, S., de Leeuw, F., Vila, J., 2004. Improvement of Classifications European Monitoring Stations for AirBase: A Quality Control.". Technical Paper 2004/7, April 2004.
Szopa, S., Hauglustaine, D.A., 2007. Relative impacts of worldwide tropospheric ozone changes and regional emission modifications on European surface-ozone levels. Compt. Rendus Geosci. 339, 709–720.
Tørseth, K., Aas, W., Breivik, K., Fjaeraa, A.M., Fiebig, M., et al., 2012. Introduction to the European Monitoring and Evaluation Programme (EMEP) and observed atmospheric composition change during 1972-2009. Atmos. Chem. Phys. 12, 5447–5481.
Traczyk, P., Gruszecka-Kosowska, A., 2020. The condition of air pollution in Kraków, Poland, in 2005–2020, with health risk assessment. Int. J. Environ. Res. Publ. Health 17, 6063, 2020.

Turner, M.C., Jerrett, M., Pope, C.A., Krewski, D., Gapstur, S.M., et al., 2016. Long-term ozone exposure and mortality in a large prospective study. Am. J. Respir. Crit. Care Med. 193, 1134–1142.

Turnipseed, A.A., Burns, S.P., Moore, D.J.P., Hu, J., Guenther, A.B., Monson, R.K., 2009. Controls over ozone deposition to a high elevation subalpine forest. Agric. For. Meteorol. 149, 1447–1459.

UNECE, United Nations Economic Commission for Europe. Convention on Long-Range Trans-boundary Air Pollution, 2010. Mapping critical levels for vegetation. In: International Cooperative Programme on Effects of Air Pollution on Natural Vegetation and Crops, Bangor, UK.

Wałaszek, K., Kryza, M., Werner, M., 2018. The role of precursor emissions on ground level ozone concentration during summer season in Poland. J. Atmos. Chem. 75, 181–204.

WHO, World Health Organisation, 2008. Health Risks of Ozone from Long-Range Transboundary Air Pollution.". WHO/Euro product. ISBN 978 92 890 42895.

WHO, World Health Organization, 2019. Global Health Estimates: Life Expectancy and Leading Causes of Death and Disability.". https://www.who.int/data/gho/data/themes/mortality-and-global-health-estimates.

Wu, R., Agathokleous, E., Feng, Z., 2021. Novel ozone flux metrics incorporating the detoxification process in the apoplast: an application to Chinese winter wheat. Sci. Total Environ. 767, 144588.

Yan, Y., Pozzer, A., Ojha, N., Lin, J., Lelieveld, J., 2018. Analysis of European ozone trends in the period 1995-2014. Atmos. Chem. Phys. 18, 5589–5605.

Zhang, Z., Jiang, J., Lu, B., Meng, X., Herrmann, H., et al., 2022. Attributing increases in ozone to accelerated oxidation of volatile organic compounds at reduced nitrogen oxides concentrations. PNAS Nexus 1, 266.

Zhang, J., Wei, Y., Fang, Z., 2019. Ozone pollution: a major health hazard worldwide. Front. Immunol., Sec. Inflammation 10. https://doi.org/10.3389/fimmu.2019.02518.